Acta Montanistica Slovaca
ISSN 1335-1788
actamont.tuke.sk

Probabilistic Model of Surface Formogenesis

Milan SAGA[1], Sergey BRATAN[2], Zuzana SAGOVÁ[3], Antastasia CHASOVITINA[4], Boris YAKIMOVICH[5], Pavol BOŽEK[6], Umer ABDULGAZIS[7] and Dilyaver ABDULGAZIS[8]*

Authors' affiliations and addresses:
[1] University of Žilina, Faculty of Mechanical Engineering, Slovakia
e-mail: milan.saga@fstroj.uniza.sk

[2] Sevastopol State University, Automation and engineering technology department, Universitetskaya 33, Sevastopol, Crimea
e-mail: serg.bratan@gmail.com

[3] University of Žilina, Faculty of Mechanical Engineering, Slovakia
e-mail: zuzana.sagova@fstroj.uniza.sk

[4] Sevastopol State University, Sevastopol, Crimea
e-mail@e-mail.com

[5] Sevastopol State University, Energy systems and complexes of traditional and renewable sources department, Universitetskaya 33, Sevastopol, Crimea
e-mail: yakimovich52@gmail.com

[6] University of Žilina, Faculty of Mechanical Engineering, Slovakia
e-mail: pavol.bozek@fstroj.uniza.sk

[7] Crimean Engineering and Pedagogical University named after Fevzi Yakubov, Motor transport department, Uchebniy alley 8, Simferopol, Crimea
e-mail: at@kipu-rc.ru

[8] Crimean Engineering and Pedagogical University named after Fevzi Yakubov, Labor protection in mechanical engineering and social sphere department, Uchebniy alley 8, Simferopol, Crimea
e-mail: ot@kipu-rc.ru

***Correspondence:**
Pavol Božek, University of Žilina, Faculty of Mechanical Engineering, Slovakia
Tel.: +421 903 240 686
e-mail: pavol.bozek@fstroj.uniza.sk

Funding information:
VEGA 1/0423/23

Acknowledgement:
This article was supported by the Scientific Grant Agency of the Slovak Republic under grant no. VEGA 1/0423/23 entitled "Experimental Research and Simulation of the Dynamic Properties of Composite Structural Elements Manufactured by 3D Printing".

How to cite this article:
Saga, M., Bratan, S., Sagová, Z., Chasovitina, A., Yakimovich, B., Božek, P., Abdulgazis, U. and Abdulgazis, D. (2025). Probabilistic Model of Surface Formogenesis. *Acta Montanistica Slovaca,* Volume 30 (3), 680-692

DOI:
https://doi.org/10.46544/AMS.v30i3.10

Abstract
In modern technological practice, the methods of abrasive diamond grinding have proven to be one of the most effective methods of surface finishing. Research conducted in the field of mechanical engineering has shown that in a number of leading countries, more than 40% of total labor costs associated with machining are concentrated on finishing operations. These operations include high-precision technologies such as diamond grinding, honing, and superfishing. According to current analytical forecasts, this share will continue to grow, underscoring the growing importance of finishing technologies in machine-building production. It is important to note that this trend is driven by the desire to improve product quality and shorten production cycles (Novoselov et al., 2017; Kassen & Werner, 1969; Malkin & Guo, 2008; Hou & Komanduri, 2003; Lajmert et al., 2018). The above operations are stochastic in nature, since during the implementation of grinding processes, the removal of the allowance from the surface of the workpiece is carried out by random flows of abrasive grains, with their quantity and density of distribution over the depth of the tool varying over time. Currently, the calculation of cutting modes is carried out according to deterministic dependencies that do not fully reflect the course of the technological process, which leads to a decrease in the productivity of technological operations and a significant variation in quality indicators. As a result, the service life of the finished product is reduced (Leonesio et al., 2012; Zhang et al., 2005; Ahrens et al., 2017; Garitaonandia et al., 2008; Tawakoli et al., 2012).

Keywords
technological process, diamond abrasive grinding, formogenesis

Introduction

The solution to the problem of increasing processing productivity while ensuring the stability of the properties of manufactured products can be found by creating a probability-theoretic theory that takes into account the dynamics of the grinding process and the stochastic properties of abrasive diamond operations (Jung et al., 2015; Yu et al., 2016; Guo, 2014; Soler et al., 2017).

Thus, to adequately predict the output parameters of these processes, it is necessary to account for both the stochastic and dynamic nature of the interaction between the tool and the part.

Authors (Sun et al., 2025) confirm that the grinding surface texture is random and feature information is weak. Increasing the efficiency of centerless grinding is discussed by Nguyen (2021). Specifically, a better grinding effect can be achieved using traditional grinding technology (Chen et al., 2022). Authors (Grigoriev et al., 2021) describe a grinding process with high cutting forces and high grinding wheel wear rates, which cause a rapid loss of dimensional accuracy and deterioration of the surface quality, while the interference of the grinding wheel with the surface being treated imposes serious limitations.

To describe the interaction between the abrasive tool and the workpiece surface, it is advisable to introduce a new technological concept: "field formogenesis". The term "field formogenesis" should be understood as the process of forming a new surface through stochastic particle flows driven by the movement of the cutting tool and the workpiece. The particle flow is characterized by a set of geometric parameters of abrasive elements at the micro and macro levels, including their number and distribution density over the tool depth.

To model the process, it is advisable to describe the position of the cutting protrusions in depth relative to a conditional outer surface, the movement of which forms a trajectory whose envelope represents a conditional boundary of the field (Majko et al., 2022).

It is convenient to consider the boundary of the effect of the shaping field on the surface to be processed in the coordinate system of the "workpiece" – from the most prominent protrusion of roughness to the maximum depth of penetration of abrasive grains into the workpiece material, and the position of the shaping elements of the field in the coordinate system of the "tool" – from the most prominent grain to the level resembling the most prominent protrusion of roughness on the surface of the workpiece.

Materials and Methods

To illustrate the above statement, consider the internal grinding process (Figures 1 and 2).

During modeling a grinding operation, the vertex of an element of the level's formative field can be specified by the coordinates y', x', z'.

Based on the scheme in question, you can write a mathematical expression:

$$y' = y_n' + W, \tag{1}$$

where y'_n – the distance from the conditional outer surface of the workpiece to the n-th level at which the material removal is calculated;

W– the distance from the deepest cavity to the midline of the profile.

The shape of the conditional field boundary for the case of internal grinding, excluding vibrations and other disturbances, is a sector with a center perpendicular to the main plane. Because the abrasive tool has deviations in roundness, vibrations are generated during the grinding process, affecting allowance removal and altering the shape of the boundary of the formogenesis field.

Taking into account the above, we can write an expression for calculating the ordinate of the points of the conditional field boundary:

$$y_n'(x,t) = y_n'(x,t_0) + \int_{t_0}^{t} V_{0y} d\tau + \Delta y_T'(x,t) + y_{yn}'(x,t) + \\ + \sum_i A_{0yi} \cos(t\omega_{0yi} + \varphi_{oyi}) \pm R(\gamma,x,t), \tag{2}$$

where $y'_n(x, t_0)$ – *the initial coordinate of the tool center position of the tool rotation*; t_0 – start time of the operation; V_{0y} – nominal feed rate of the tool in the radial direction according to the coordinate y;

$\Delta y_T'(x,t)$, $y_{yn}'(x,t)$ – deformation of the boundary of the formogenesis field due to elastic and temperature processes occurring in the contact zone (Kopas et al., 2017);

A_{yi} – the amplitude, ω_{yi}– frequency, φ_{yi}– the phase of harmonic pulsations of the position of the center of rotation of the instrument for the i-th harmonics.

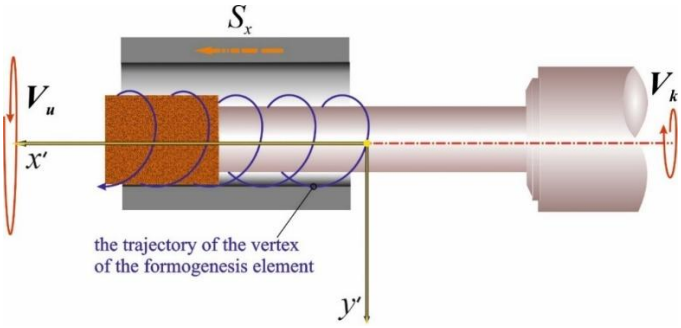

Fig. 1. Formogenesis during internal grinding

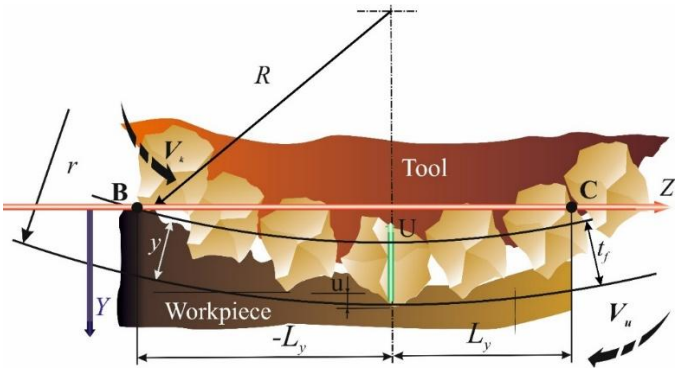

Fig. 2. Contact zone BC on the section [-L_Y; L_Y]of the workpiece surface with a radius r with an abrasive tool of radius R

For analysis, we will select a basic surface area on which the tool grains move parallel to themselves in the contact zone, and then the coordinates of the points of the cutting surface will be determined as:

$$\left.\begin{aligned} z &= z_0 + \int_{t_0}^{t}\left[R(M)\omega_k\cos\gamma + V_{0z} + V_{0Az} + V_{oynz} + V_{ozg} + V_{3z}\right]dz;\\ y &= y_0 + \int_{t_0}^{t}\left[R(M)\omega_k\cos\gamma + V_{0y} + V_{0Ay} + V_{oyny} + V_{oyg} + V_{3y}\right]dy;\\ x &= x_0 + \int_{t_0}^{t}\left[R(M)\omega_k\cos\gamma + V_{0x} + V_{0Ax} + V_{oynx} + +V_{oxg} + V_{3x}\right]dx; \end{aligned}\right\}, \tag{3}$$

Where *R(M)* – radius is the vector of the farthest point of the abrasive tool;

ω – angular velocity of the tool; z_0, y_0, x_0– coordinates that determine the position of the cutting edge of the tool at the initial moment of time t_0; γ – the angle between the radius vector of the outermost point of the abrasive tool and the axis *z*; V_{0Az}, V_{0Ay}, V_{0Ax} – projections of the speed of movement of the tool axis in the presence of vibrations in the contact area of the abrasive tool and the workpiece;

V_{oynz}, V_{oyny}, V_{oynx} – projections of the velocity of the tool axis in the presence of elastic deformations in the contact zone of the abrasive tool and the workpiece;

V_{0zg}, V_{0yg}, V_{0zg} – projections of the velocity of the tool axis in the presence of temperature deformations in the contact zone of the abrasive tool and the workpiece;

V_{3z}, V_{3y}, V_{3x} – projections of the rate of change of the edge coordinates relative to the center of the tool during its elastic deformation.

The system of equations (2) contains both deterministic and random variables, so the shape of the surfaces formed as a result of the action of the formogenesis field on the workpiece material will be random.

While studying the laws governing the distribution of cutting edges across the depth of an abrasive tool, mathematical expressions from the theory of precision processing of materials can be used.

During grinding, the surface of the workpiece is formed by the stochastic interaction of abrasive elements with the workpiece material (Novoselov et al., 2017).

The technological process parameters and their outputs depend on the number of cutting elements in the contact zone between the abrasive tool and the workpiece.

For example, in abrasive grinding operations, the number of elements of the formogenesis field nn(lx,lz) can be determined by the number of abrasive grains per unit volume or area of the tool. The number of such edges is calculated based on:

$$n_n(l_x,l_z) = n_3 l_x l_z \frac{V_k}{V_u} i \quad npu \quad l_x = l_z = 1; n_n = n_3 \frac{V_k}{V_u}, \tag{4}$$

where i – the number of contacts between the surface area of the tool and the surface area of the workpiece.

For the X and Z coordinate axes, if there are deviations in the values of the tool and workpiece speeds, the distribution of elements may be uneven. Probability density $f_{\eta z(t)}(z)$ of distances η_z along the Z axis from the origin of the coordinate system to the vertices of the elements can be calculated as:

$$f_{\eta z}(z) = \frac{1}{n_n(l_x,l_z)} \cdot \frac{dn_n(l_x,l_z)}{dz}. \tag{5}$$

The number of elements of the base section of the field, taking into account changes in the speed of the tool $V_k(\tau)$ and workpiece speed $V_u(\tau)$:

$$n_n(l_x,l_z) = n_3 l_x \int_0^{l_z} \frac{V_k(\tau)}{V_u(\tau)} dz(\tau) \tag{6}$$

can be determined using the Stieltjes integral, then the probability density can be calculated using the formula:

$$f_{\eta z}(z) = \frac{V_k(\tau)}{V_u(\tau) \int_0^{l_z} \frac{V_k(\tau)}{V_u(\tau)} dz(\tau)}. \tag{7}$$

The displacement of the position of the cutting edges in the workpiece material can be described in the coordinate system of the tool. For example, the value of the u-distance from the conditional outer surface of the tool to the level in the working layer of the tool in the direction of the radius vector can be calculated:

$$u(t) = y' - y'_u(t_0) + \int_{t_0}^{t} V_y d\tau, \tag{8}$$

where y'_u– the coordinate of the conditional boundary of the formogenesis field.

Based on expression (8), a dependence can be obtained for calculating the instantaneous probability density of the vertices of the field $f_{\eta y(t)}(y')$along the y axis:

$$f_{\eta y(t)}(y') = f_{\xi u}(y' - y'_u(t_0) + \int_{t_0}^{t} V_y d\tau). \tag{9}$$

For the average values of the densities of instantaneous distributions, expression (10) is rewritten:

$$f_{\eta y'}(y') = \frac{1}{t_1 - t_0} \int_{t_0}^{t_1} f_{\xi u}(y' - y'_u(t_0) + \int_0^t V_y d\tau) dt. \tag{10}$$

Considering the feed values S_{yi} and the number of grains per unit surface of the grinding tool n_{gi} for passes from the first to m, the density for discrete movement will be calculated using the formula:

$$f_{\eta y'}(y') = \frac{1}{n_{g1} + n_{g2} + \ldots + n_{gm}} \times \times \left[\begin{array}{l} n_{g1} f_{\xi u}(y' - y'_u + S_y) + n_{g2} f_{\xi u}(y' - y'_u + S_{y1} + S_{y2}) + \\ + \ldots + n_{gm} f_{\xi u}(y' - y'_u + \sum_{i=1}^{m} S_{yi}) \end{array} \right], \quad (11)$$

In most cases, the grinding process consists of multi-pass sections, and several extreme values of probability density are observed for such processing (Figure 3).

The analysis of the field of Formogenesis

The working surface can also be described in another way, in which the elementary cutting profiles are independent components of the formogenesis process.

If the distance distribution functions of the points of elementary profiles are known, then the ordinate function of the profile is probabilistic in nature, and the ordinate Y of the profile point is obtained below the set value (Figure 4):

$$F_y(y') = 1 - [1 - F_U(W - W_1)][1 - F_U(W - W_2)]..[1 - F_U(W - W_K)], \quad (12)$$

Where W_1, W_2, ... W_k– the distances from the conditional field boundary to the conditional outer surface of the tool at the moment of passing through sections 1,2, ..., K of elementary cutting profiles.

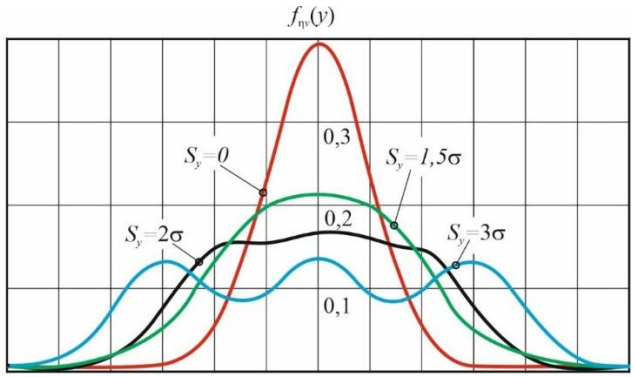

Fig. 3. Dependence of the density of the cutting surface distribution on the radial feed

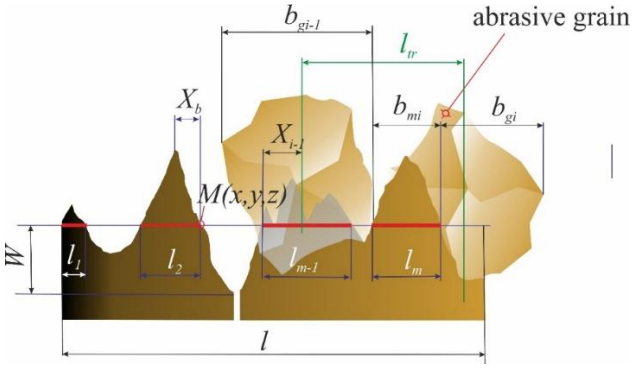

Fig. 4. Diagram for the analysis of the field of formogenesis

Due to the formogenesis of the field, it is incorrect to consider the grinding process as an ideal geometric reproduction of the particle flow. The elements of the formogenetic field, when in contact with the treated surface, can initiate various processes, including mechanical cutting, plastic deformation, and others. In this regard, we

will use the concept of the probability of material removal and non-removal at an arbitrarily selected point *M(x,y,z)*. According to the axioms of probability theory, the sum of the probabilities of mutually exclusive events is equal to one, which in this context is reflected in the corresponding mathematical relation. Therefore, the probability of an event is determined by the position of a point in the coordinate system or by changes in individual coordinates (Novoselov et al., 2017).

In particular, if the point is located in the range of the roughness protrusion, then the probability of removing material at this point tends to zero; in the opposite case, to unity. Under the conditions of the stationary profile of the treated surface and the absence of rigid fixation relative to the origin, the graph of the probability of material removal is approximated by a straight line parallel to the abscissa axis, and its quantitative estimate is calculated as the ratio of the sum of the lengths of the grain width segments b_{Mi}, containing the removed material to the total length of the section *l* (Bratan et al., 2021).

$$P(M) = 1 - P(\overline{M}) = 1 - \lim_{l \to \infty} \frac{\sum_i b_{Mi}}{l}. \tag{13}$$

Due to the fact that $l \to \infty$ Due to the fact that the sum of the profiles of the abrasive grains passed through the cross section can be replaced by the formula $\Sigma b_{Mi} \to l\lambda M[b_M]$, therefore, the probability of material removal can be defined as:

$$P(M) = 1 - \lambda M\left[b_M\right], \tag{14}$$

Where λ is the mathematical expectation of the number of projections per unit section length.

For various combinations of X and Z coordinates, the Y coordinate can be determined, with the probability of material removal fixed at β_M.

The resulting set of such points will form a surface in space, and when it is cross–sectional, the functional dependencies of material removal will appear.

The maximum value of the material removal probability $\beta_{M\,max}$ cannot be more than one, and the minimum value $\beta_{M\,min}$ less than zero. Between the specified boundaries "above and below", you can select a limited area of the material-environment.

By changing the position of the levels of equal probability, it is possible to judge the spatial deviations of the treated surface and the change in the size of the layer in which the surface roughness is distributed (Figure 5).

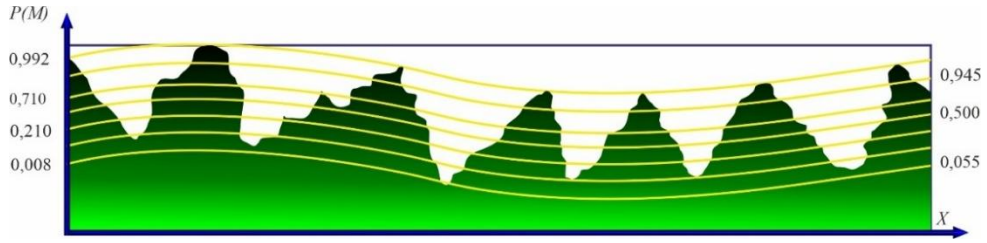

Fig. 5. The position of the levels of equal probability on the treated surface

The material removal probability parameter can be determined at any point in the space of the treated surface, and the probability functional describes this surface as a random field.

If the profile is not rigidly fixed, then at the point with coordinates (0;0), there is a coincidence of the functional and the density function of the ordinate distribution of the profile of the part. $F_w(W)$. The distribution density function itself is defined as the probability when:

$$F_W(W) = P(W < w). \tag{15}$$

where *W is* the set value of a random variable *W*.

Let the probability of a point falling into the intervals (Figure 6) be numerically equal to the width of a random grain when $W<w$, then the probability of any arbitrary surface profile can be defined as:

$$P(W < w) = \lim_{l \to \infty} \frac{l - \sum_{i} b_{Mi}}{l} = P(M). \tag{16}$$

If the reproducing field is completely reflected or copied onto the surface of the part, then the probability of removing the material:

$$P(M) = F_W(W). \tag{17}$$

Accordingly, if one of the processes dominates, then the described parameters must be determined based on the parameters of the reproducing field.

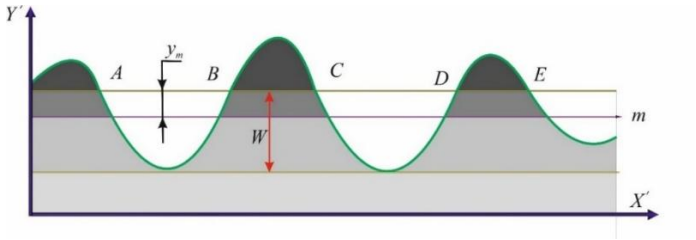

Fig. 6. Calculation scheme

Given that several processes simultaneously affect formogenesis, when calculating the probability of material removal, it is necessary to account for the nature of their combination. Processes during formogenesis can be accompanied by both:

- mutual oscillations of the tool and the workpiece (Bratan & Chasovitina, 2023; Bratan et al., 2022);
- brittle fracture (chipping) during the processing of ceramics and sitalls (Bratan et al., 2021);
- waves of plastic deformation (Bratan & Chasovitina, 2022), etc.

To assess the impact of the described events on the probability of material removal during internal grinding of workpieces, a series of experiments were conducted on a CNC machine mod. RSM M 500B (Figure 7a, 7b) and the corresponding profilograms were obtained (Figures 8, 9, 10). The roughness of the treated surface was measured using a Mitutoyo Surftest SJ-210 profilometer. To determine surface undulation, profilometers (profilographs) of models 201 and Talysurf 5M-120 were used. Mechanical roughness filtration was used to construct the waveforms.

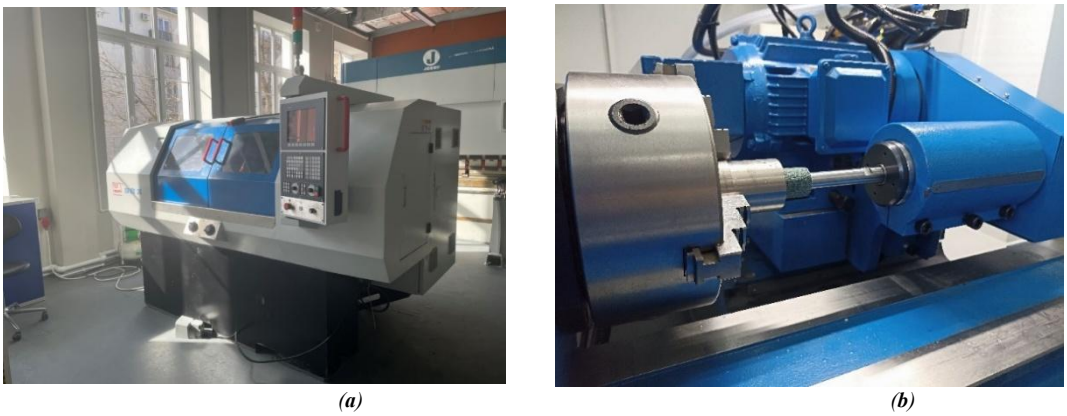

(a) ***(b)***

Fig. 7. ***(a)*** *General view of the CNC machine mod. RSM M 500B;* ***(b)*** *The internal grinding process*

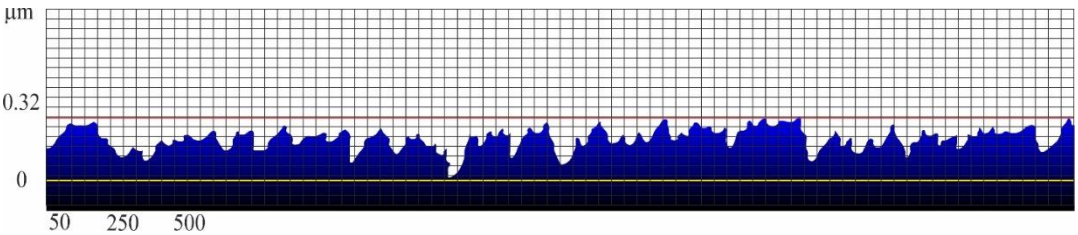

Fig. 8. Profilogram of a polished titanium alloy surface

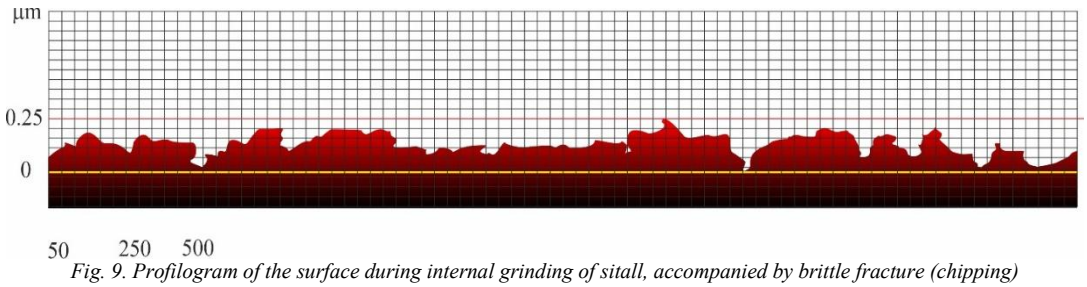

Fig. 9. Profilogram of the surface during internal grinding of sitall, accompanied by brittle fracture (chipping)

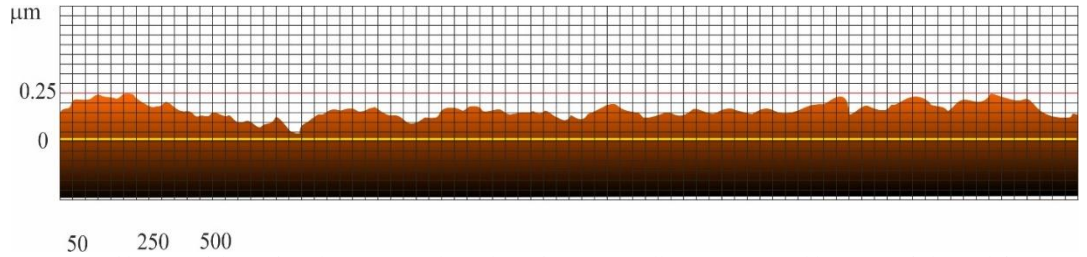

Fig. 10. Profilogram of the surface during internal grinding of a titanium alloy, accompanied by waves of plastic deformation

In most cases, the processes of abrasive and combined grinding are dependent on each other, for example, in electrochemical grinding. It simultaneously causes both mechanical destruction, electrochemical dissolution, and electroerosive destruction. If we consider the sequence of operations performed in a given technological process (for example, turning is performed first, then grinding), then such processes are independent. To determine the probability of deletion in dependent and independent processes, it is necessary to refer to probability theory.

Results

In the conditions of dependent events, illustrated by the process of grinding a thread with a multi-thread tool with a tool offset along the generatrix (Figure 11), the probability of material removal is determined by the probability of an event in which an arbitrarily selected point is located within the geometric profile of the tool, determined either by the second pass, or the first pass, or a combination of the first and second passes:

$$P(M_1 + M_2) = P(M_1) + P(M_2) - P(M_1 M_2), \tag{18}$$

where $P(M_1 M_2)$ – the probability of completing a joint event.

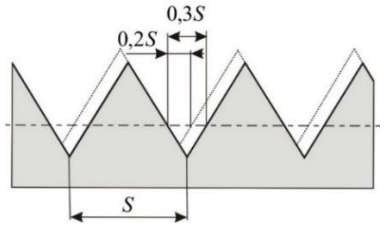

Fig. 11. Scheme for calculating the probability of material removal during grinding a thread with a multi-thread tool

If the events are independent:

$$P(M_1 + M_2) = 1 - P(\overline{M}_1)P(\overline{M}_2). \tag{19}$$

In the case of grinding of sitalls, the probability of material removal in different sections z of the length of the contact zone L_y on the different levels y contains two independent events – the removal of the material due to mechanical processing and the removal of the material due to brittle fracture (Table 1, Figure 12 (Bratan et al., 2021)).

Tab. 1. Probability of material removal at various levels during the crushing of brittle materials

z	y								
	y=0,1·tf	y=0,2·tf	y=0,3·tf	y=0,4·tf	y=0,5·tf	y=0,6·tf	y=0,7·tf	y=0,8·tf	y=0,9·tf
–6,76	0,998	0,993	0,98	0,95	0,895	0,806	0,687	0,559	0,459
–5,07	1	0,999	0,999	0,994	0,975	0,92	0,806	0,642	0,486
–3,38	1	1	1	0,999	0,994	0,967	0,88	0,71	0,512
–1,69	1	1	1	1	0,999	0,986	0,926	0,764	0,536
0	1	1	1	1	1	0,994	0,954	0,809	0,56
1,69	1	1	1	1	1	0,998	0,972	0,845	0,582
3,38	1	1	1	1	1	0,999	0,983	0,874	0,603
5,07	1	1	1	1	1	1	0,989	0,898	0,623
6,76	1	1	1	1	1	1	0,993	0,917	0,642

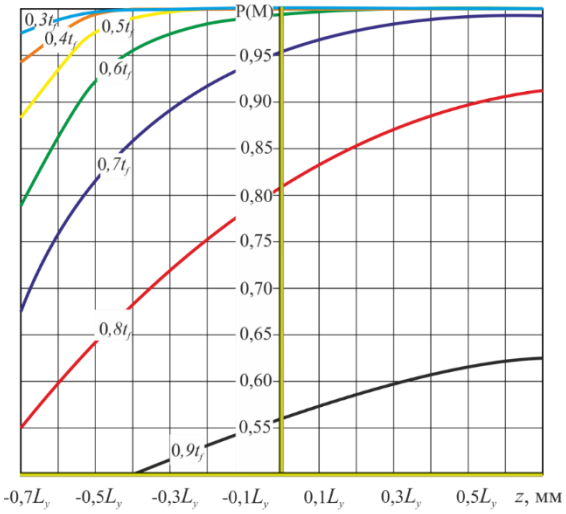

Fig. 12. The probability of material removal at various levels during the grinding of brittle materials

Conclusions

During the final grinding of titanium, during the event of mechanical removal of the material, which takes into account the mutual vibrations of the workpiece and the tool at different frequencies, the values of the probability of material removal are shown in Table 2, and the graph of the probability change is shown in Figure 13 (Bratan & Chasovitina, 2023; Bratan et al., 2022).

Tab. 2. Probability of material removal at various levels during grinding brittle materials at a frequency of 100 Hz

y = 0,3.tf, м		**y = 0,6.tf, м**		**y = 0,9.tf, м**	
z, м	P(M)	z, м	P(M)	z, м	P(M)
-0,36	0,925	-0,27	0,769	-0,14	0,576
-0,27	0,977	-0,20	0,853	-0,11	0,608
-0,18	0,995	-0,14	0,914	-0,07	0,639
-0,09	0,999	-0,07	0,953	- 0,03	0,669
0	1	0	0,976	0	0,698
0,09	1	0,07	0,988	0,03	0,724
0,18	1	0,014	0,994	0,07	0,749
0,27	1	0,20	0,997	0,11	0,770
0,36	1	0,27	0,999	0,14	0,788

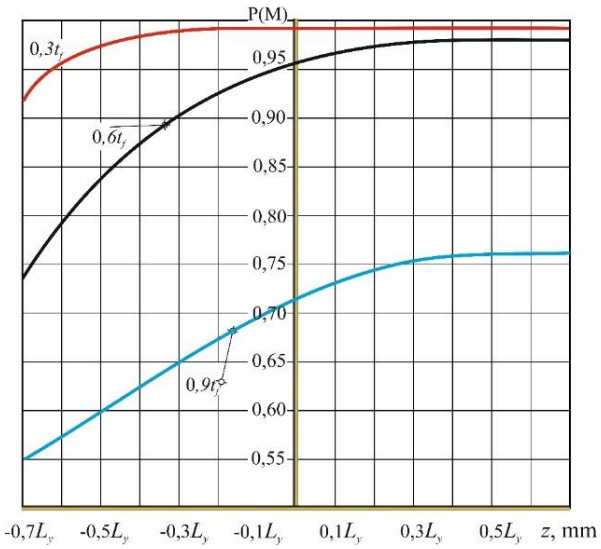

Fig. 13. The probability of material removal at various levels during grinding brittle materials at a frequency of 100 Hz

In the case of the formogenesis of the surface, accompanied by waves of plastic deformation during the processing of parts made of titanium and titanium alloys, the probability of material removal influenced by the chip formation coefficient K_c , which is not a constant value in real processing conditions (Table 3, Figure 14) (Bratan & Chasovitina, 2022).

Tab. 3. Values of the probability of material removal during grinding holes in blanks made of titanium alloys, accompanied by waves of plastic deformation

z	K_C = constant			K_C = variable		
	levels y					
	$y = 0{,}25.t_f$	$y = 0{,}50.t_f$	$y = 0{,}75.t_f$	$y = 0{,}25.t_f$	$y = 0{,}50.t_f$	$y = 0{,}75.t_f$
−0,8(L_y/2)	0,954	0,761	0,48	0,922	0,709	0,461
−0,6(L_y/2)	0,994	0,88	0,542	0,987	0,833	0,51
−0,4(L_y/2)	0,999	0,942	0,591	0,99	0,915	0,559
−0,2(L_y/2)	1	0,968	0,645	0,991	0,95	0,61
0	1	0,989	0,683	1	0,974	0,642
0,2(L_y/2)	1	0,997	0,719	1	0,981	0,670
0,4(L_y/2)	1	0,998	0,752	1	0,99	0,701
0,6(L_y/2)	1	0,999	0,78	1	0,995	0,734
0,8(L_y/2)	1	0,999	0,809	1	0,999	0,767

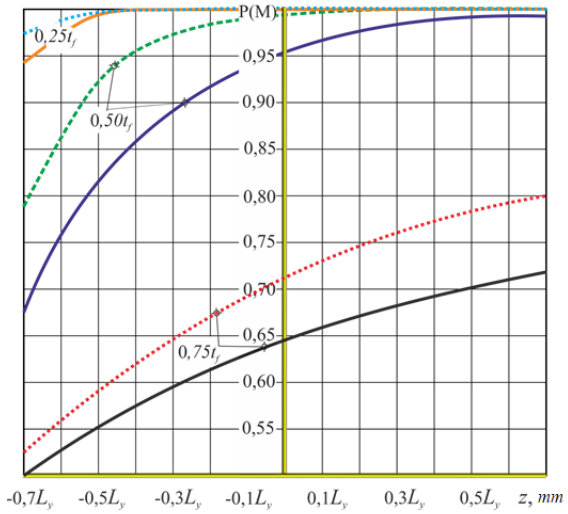

Fig. 14. The probability of material removal during grinding holes in titanium alloy blanks without and accompanied by waves of plastic deformation

If in several processes, in the case of an increase in the amount of material at a given level due to the occurrence of one of them, it is advisable to consider the possibility of non-removal of the material:

$$P\left[(\overline{M})+\overline{M}^{*})\right]=P(\overline{M})+P(\overline{M}^{*})-P(\overline{M}\,\overline{M}^{*}), \tag{20}$$

where $P(\bar{M}^{*})$ is the probability of an increase in the proportion of material at a fixed point.
For dependent simultaneous processes, with any number of them, the probability of material removal can be calculated as:

$$\begin{aligned}P(M)=P\left[\sum_{i}^{m}\overline{(M_i+\overline{M_i}^{*})}\right]=\sum_{i}P\overline{(M_i+\overline{M_i}^{*})}-\sum_{ij}P\left[\overline{(M_i+\overline{M_i}^{*})}\,\overline{(M_j+\overline{M_j}^{*})}\right]+\\+\sum_{ijk}P\left[\overline{(M_i+\overline{M_i}^{*})}\,\overline{(M_j+\overline{M_j}^{*})}\,\overline{(M_k+\overline{M_k}^{*})}\right]-\ldots+\\+(-1)^{m-1}P\left[\overline{(M_1+\overline{M_1}^{*})}\times\overline{(M_2+\overline{M_2}^{*})}\ldots\overline{(M_m+\overline{M_m}^{*})}\right].\end{aligned} \tag{21}$$

For independent processes:

$$P\left[\sum_{i=1}^{m}\overline{(M_i+\overline{M_i}^{*})}\right]=1-\prod_{i=1}^{m}P(\overline{M_i}+\overline{M_i}^{*}). \tag{22}$$

The resulting equations can be easily verified by geometric constructions. For example, for dependent events (thread grinding with a multi-thread tool), equation (15) is valid.
When $i=2$, $b_{M1}=S-0{,}2S$; $b_{M2}=S-0{,}3S$, the probability can be calculated as:

$$\begin{aligned}&P(M_1)=1-\frac{S-0{,}2S}{S}=0{,}2, P(M_2)=0{,}3; P(M_1M_2)=0{,}2;\\&P(M_1+M_2)=0{,}2+0{,}3-0{,}2=0{,}3;\end{aligned} \tag{23}$$

If several factors of the formogenesis affect the parts, which ensure the removal of material from it, the overall probability of this event is equal to the probability that all the individual, simplest factors combined will work.

In cutting theory, from the perspective of creating a machined surface, we talk about the following factors: copying the shape of the cutting tool into the workpiece, copying the roughness of the cutting edges themselves, the formation of growth (BUE – Built-up Edge, and wear. These are factors for cutting tools with a defined cutting edge (Peterka, 2004; Polakovic et al., 2008; Vopát et al., 2014). Another significant factor, which is also present in processes with an undefined cutting edge - where individual cutting wedges are randomly distributed in the volume of material (such as grinding, lapping, superfinishing, etc.) - are vibrations (Silva et al., 2023), which are clearly of a random nature.

To calculate the probability of material removal and determine what the treated surface will look like, the following calculation sequence can be proposed. We divide a complex process into simple components. First, we find how the heights of the irregularities created by each simple process are distributed (using the ordinate distribution function, equation 8), and the probability of material removal (equation 11). Then, using these data, we determine the overall probability of removing the material from the entire complex of processes (Equation 15). Knowing this general probability, we can calculate the distribution of the heights of the irregularities on the final machined surface of the part (Equation 11).

In future research, it would be appropriate to use this equation for other similar processes besides grinding, for instance, rum (Kuruc et al., 2014; Kuruc et al., 2013), drag finishing (Peterka et al., 2020; Pokorny et al., 2020; Peterka et al., 2020), or superfinishing (Lipa et al., 2012; Görög, 2021), etc., where there is a lot of experimental data, for their comparison.

References

Ahrens, M., Damm, J., Dagen, M., Denkena, B., & Ortmaier, T. (2017). Estimation of dynamic grinding wheel wear in plunge grinding. Procedia CIRP, 58, 422–427. https://doi.org/10.1016/j.procir.2017.03.247

Bratan, S. M., & Chasovitina, A. S. (2022). Influence of plastic deformations on the process of material removal during finishing grinding of titanium alloys. *Scientific Notes of the Crimean Engineering Pedagogical University*, 4(78), 237–243. https://doi.org/10.34771/UZCEPU.2022.78.4.047

Bratan, S. M., & Chasovitina, A. S. (2023). Simulation of the relationship between input factors and output indicators of the internal grinding process, considering the mutual vibrations of the tool and the workpiece. *Metal Working and Material Science*, 25, 57–70. https://doi.org/10.17212/1994-6309-2023-25.1-57-70

Bratan, S. M., Roshchupkin, S. I., Chasovitina, A. S., & Gupta, K. (2022). The effect of the relative vibrations of the abrasive tool and the workpiece on the probability of material removing during finishing grinding. *Metal Working and Material Science*, 24(1), 33–47. https://doi.org/10.17212/1994-6309-2022-24.1-33-47

Bratan, S. M., Roshchupkin, S. I., Kharchenko, A. O., & Chasovitina, A. S. (2021). Probabilistic model of surface layer removal when grinding brittle non-metallic materials. *Metal Working and Material Science*, 23, 6–16. https://doi.org/10.17212/1994-6309-2021-23.2-6-16

Chen, C., Chen, B., Wu, C., Gu, X., Liu, X., & Guo, F. (2022). [Article title not provided]. *Metals*, 12(7), 1209. https://doi.org/10.3390/met12071209

da Silva, W. T. A., Peterka, J., & Vopat, T. (2023). Experimental research on the dynamic stability of internal turning tools for long overhangs. *Journal of Manufacturing and Materials Processing*, 7(2). https://doi.org/10.3390/jmmp7020061

Garitaonandia, I., Fernandes, M. H., & Albizuri, J. (2008). Dynamic model of a centerless grinding machine based on an updated FE model. International Journal of Machine Tools and Manufacture, 48, 832–840. https://doi.org/10.1016/j.ijmachtools.2007.12.001

Görög, A. (2021). Simulation of superfinished surface formation. *Advances in Science and Technology Research Journal*, 15(2), 219–227. https://doi.org/10.12913/22998624/133064

Grigoriev, S. N., Nadykto, A. B., Volosova, M. V., Zelensky, A. A., & Pivkin, P. M. (2021). [Article title not provided]. *Metals*, 11(6), 882. https://doi.org/10.3390/met11060882

Guo, J. (2014). Surface roughness prediction by combining static and dynamic features in cylindrical traverse grinding. *International Journal of Advanced Manufacturing Technology*, 75, 1245–1252. https://doi.org/10.1007/s00170-014-6189-5

Hou, Z. B., & Komanduri, R. (2003). On the mechanics of the grinding process. Part 1. Stochastic nature of the grinding process. International Journal of Machine Tools and Manufacture, 43, 1579–1593. https://doi.org/10.1016/S0890-6955(03)00186-X

Jung, J., Kim, P., Kim, H., & Seok, J. (2015). Dynamic modeling and simulation of a nonlinear, non-autonomous grinding system considering spatially periodic waviness on workpiece surface. *Simulation Modelling Practice and Theory*, 57, 88–99. https://doi.org/10.1016/j.simpat.2015.06.005

Kassen, G., & Werner, G. (1969). Kinematische Kenngrößen des Schleifvorganges [Kinematic parameters of the grinding process]. Industrie-Anzeiger, 87, 91–95. (In German).

Kopas, P., Saga, M., Baniari, V., Vasko, M. & Handrik, M. (2017). A plastic strain and stress analysis of bending and torsion fatigue specimens in the low-cycle fatigue region using the finite element methods. XXI POLISH-SLOVAK SCIENTIFIC CONFERENCE MACHINE MODELING AND SIMULATIONS MMS 2016, Volume 177, Page 526-531, DOI10.1016/j.proeng.2017.02.2

Kuruc, M., Vopát, T., & Peterka, J. (2014). Surface roughness of polycrystalline cubic boron nitride after rotary ultrasonic machining. *Procedia Engineering*, 100, 877–884. https://doi.org/10.1016/j.proeng.2015.01.444

Kuruc, M., Zvončan, M., & Peterka, J. (2013). Investigation of ultrasonic assisted milling of aluminum alloy AlMg4.5Mn. *Procedia Engineering*, 69, 1048–1053. https://doi.org/10.1016/j.proeng.2014.03.089

Lajmert, P., Sikora, V., & Ostrowski, D. (2018). A dynamic model of cylindrical plunge grinding process for chatter phenomena investigation. MATEC Web of Conferences, 148, 09004. https://doi.org/10.1051/matecconf/20181480900

Leonesio, M., Parenti, P., Cassinari, A., Bianchi, G., & Monn, M. (2012). A time-domain surface grinding model for dynamic simulation. Procedia CIRP, 4, 166–171. https://doi.org/10.1016/j.procir.2012.10.030

Lipa, Z., Görög, A., Bartoš, R., & Kolník, M. (2012). The research of a surface roughness after the superfinishing. In *International Doctoral Seminar 2012: Proceedings*, Smolenice Castle, Slovakia, May, 288–294. ISBN 978-80-8096-164-0.

Majko, J., Vasko, M., Handrik, M. & Saga, M. (2022). Tensile Properties of Additively Manufactured Thermoplastic Composites Reinforced with Chopped Carbon Fibre. MATERIALS, Volume 15, Issue 12. DOI10.3390/ma15124224

Malkin, S., & Guo, C. (2008). Grinding technology: Theory and applications of machining with abrasives (2nd ed.). Industrial Press. ISBN 978-0-8311-3247-7.

Nguyen, A. T. (2021). Multi-objective optimization of process parameters to enhance efficiency in the shoe-type centerless grinding operation for internal raceway of ball bearings. *Metals*, 11(6), 893. https://doi.org/10.3390/met11060893

Novoselov, Y., Bogutsky, V., & Shron, L. (2017). Patterns of removing material in workpiece–grinding wheel contact area. Proceedings of the International Conference on Industrial Engineering (ICIE 2017), Saint Petersburg, Russia, 16–19 May 2017. Elsevier. pp. 991–996. https://doi.org/10.1016/j.proeng.2017.10.583

Peterka, J. (2004). A new approach to calculating the arithmetical mean deviation of a profile during copy milling. *Strojniski Vestnik/Journal of Mechanical Engineering*, 50(12), 594–597. ISSN 0039-2480.

Peterka, J., Pokorny, P., Vaclav, S., Patoprsty, B., & Vozar, M. (2020). Modification of cutting tools by drag finishing. *MM Science Journal*, March, 3822–3825. https://doi.org/10.17973/MMSJ.2020_03_2019130

Peterka, J., Vozar, M., Vopat, T., Pokorny, P., & Patoprsty, B. (2020). [Article title not provided]. *Materials Today: Proceedings*, 22, 205–211. https://doi.org/10.1016/j.matpr.2019.08.089

Pokorny, P., Patoprsty, B., Vopat, T., & Peterka, J. (2020). [Article title not provided]. *Materials Today: Proceedings*, 20, 212–218. https://doi.org/10.1016/j.matpr.2019.08.090

Polakovic, M., Buransky, I., & Peterka, J. (2008). *Annals of DAAAM for 2008 and 19th International DAAAM Symposium "Intelligent Manufacturing and Automation: Focus on Next Generation of Intelligent Systems and Solutions"*, 1089–1090. ISSN 1726-9679.

Soler, Ya. I., Le, N. V., & Si, M. D. (2017). Influence of rigidity of the hardened parts on forming the shape accuracy during flat grinding. *MATEC Web of Conferences*, 129, 01076. https://doi.org/10.1051/matecconf/201712901076

Sun, F., Yi, H., & Wang, H. (2025). Visual measurement of grinding surface roughness based on GE-MobileNet. *Applied Sciences*, 15(21), 11489. https://doi.org/10.3390/app152111489

Tawakoli, T., Reinecke, H., & Vesali, A. (2012). An experimental study on the dynamic behavior of grinding wheels in high-efficiency deep grinding. Procedia CIRP, 1, 382–387. https://doi.org/10.1016/j.procir.2012.04.068

Vopát, T., Peterka, J., Simna, V., & Kuruc, M. (2014). The influence of different types of copy milling on the surface roughness and tool life of end mills. *Procedia Engineering*, 100, 868–876. https://doi.org/10.1016/j.proeng.2015.01.443

Yu, H., Wang, J., & Lu, Y. (2016). Modeling and analysis of dynamic cutting points density of the grinding wheel with an abrasive phyllotactic pattern. *International Journal of Advanced Manufacturing Technology*, 86, 1933–1943. https://doi.org/10.1007/s00170-015-8262-0

Zhang, N., Kirpitchenko, I., & Liu, D. K. (2005). Dynamic model of the grinding process. Journal of Sound and Vibration, 280, 425–432. https://doi.org/10.1016/j.jsv.2003.12.006